Fatigue Behavior of Crack Initiating from Corrosion Damage

M. Khobaib, T. Matikas, and M.S. Donley
Air Force Research Laboratory
Wright-Patterson AFB, OH

Received 08/20/01; Revised manuscript received 03/12/02

Abstract

The initiation and growth of fatigue crack emanating from corrosion pits was investigated by conducting fatigue experiments on standard dog-bone specimens of high strength aluminum alloy AA2024–T3. The corrosion pits were created in an electrochemical cell under specific polarization conditions. Samples were prepared with varying pit depth and pits were initially characterized using a white light interferometer. The fractured surface was analyzed under scanning electron microscope after the fatigue test. These cracks were treated as surface cracks for stress intensity calculations. A linear relationship between stress intensity factor and critical pit depth was observed. The crack growth behavior of the crack nucleating from these pits was typical of a short crack.

Introduction

The United States Air Force has a large fleet of aging aircraft, which is expected to grow further due to budgetary restrictions. Most of these aircraft will be in operation for longer than they were originally designed to be[1]. For example, the C/KC-135, which was produced in 1950's and 1960's, is currently projected for service through the first half of the 21st century[2]. These aircraft are now limited by their "corrosion lifetime" rather than their "fatigue lifetime". The older these aircraft get, the maintenance of their structural integrity becomes increasingly critical for life sustainment. Hence, increased attention is required towards structural damage modeling, repair and life prediction.

One of the main causes of failure of aging aircraft is corrosion damage, fatigue cracking and their synergistic interactions. Since corrosion is a time dependent process, these problems are bound to worsen with the continued service use of these aircraft. These issues are being addressed with research initiatives to define the corrosion problem facing aging aircraft, perform structural testing and studies, and developing analytical tools for qualifying the effects of corrosion on structural integrity[3].

Several excellent articles deal with corrosion and its effects on aircraft structural integrity[4,5]. Research has shown that pits are one of the nucleation sites of fatigue crack formation in aluminum alloys[6-8]. Continued growth of these cracks under fatigue results in premature failure of the aircraft structure.

Pitting has been recognized as the cause of fatigue crack initiation in several aircraft structural failures. The loss of Aloha Airlines aircraft during flight and the failure of the trailing edge flap hinge of an Australian F/A-18, which lost its flap during flight are documented as failures resulting from fatigue cracks initiating from pits[9]. Extensive intergranular cracking has been observed to emanate from severe pitting in the bores and countersink areas of fastener holes in the wing box lower panel of a fighter aircraft[10]. Quantitative measures such as pit dimensions and surface roughness as corrosion metrics have been used along with crack growth tools in estimating fatigue life of components subjected to corrosion[11]. Other studies have focused on measuring and applying a large number of candidate metrics for quantifying corrosion in aging KC-135[12].

This study was initiated under the sponsorship of Department of Defense, to quantitatively investigate the role of corrosion damage on the fatigue behavior of high strength aluminum alloys. It must be emphasized that the pitting effect on fatigue is not yet well understood. A large number of laboratory investigations have studied the effects of prior corrosion and the presence of a corrosive environment on fatigue crack initiation and growth of high strength aluminum alloys[4, 5]. These studies, however, have not addressed the early stages of corrosion and its transition to fatigue cracking in structural materials. The information presented in this study about short-term

as well long-term effects of corrosion is vital to understanding the early stages of damage evolution in aircraft structure whose operational mechanical and environmental spectra are not adequately represented in laboratory experiments. Nakajima and Tokaji[13] have found that a crack emanates from a pit during simultaneous corrosion fatigue only if the pit grows to the level when the stress intensity factor reaches a certain threshold value. Phillips and Neuman[14] demonstrated that the fracture mechanics of long crack fatigue growth in AA2024-T3 alloy leads to substantial exaggeration of the fatigue life for a very small initial size.

In this study, controlled pits were grown electrochemically in standard dog-bone fatigue samples, which were then tested under fatigue condition in laboratory air. The primary objective of this study is to develop a relationship between a pitting parameter and a structural integrity parameter. The overall objective is to formulate a life prediction model based on pitting parameters obtained from nondestructive evaluation tool used in the service and expected fatigue spectra of the aircraft.

Experimental

Standard dog–bone fatigue samples of AA2024-T3 were machined having the tensile axis parallel to the rolling direction. The dimensions for the fatigue specimens are (Figure 1). Each sample was cleaned and prepared at a time. The gage section of the sample was sanded up to 600 grit SiC paper. The sample was then rinsed with distilled water and dried with a stream of air. Most of the specimen's surface was covered with a waterproof tape. A small portion in the center of the gage section was initially left exposed as shown in (Figure 1), and later covered with a thin coat of micro-stop. A fine hole was created in the microstop coating after the film had dried. This was intentionally done to provide desired site/sites for pit initiation. The sample thus prepared was glued into an electrolytic cell for electrochemically producing pit/pits on the surface. A solution of 0.1 M NaCl was used as the pitting electrolyte. A saturated calomel electrode (SCE) was used as the reference while platinum meshed disc served as the counter electrode. The pitting was produced in the area of the exposed gage section using a potentiostatic scan. An initial potential of -450 mV (SCE) was applied for 10 minutes, and then the potential was lowered to -520 mV (SCE) for the remainder of the scan. Various scan times were used to obtain pits of varying depth. The sample was promptly removed from the cell, after the potential scan, cleaned with running distilled water and dried in a stream of air. The pit morphology and depth measurements were determined using optical microscopy[15].

The pit morphology and depth measurements were determined using optical microscopy, SEM and WLIM. The samples were then fatigued within 24 hours of being removed from the electrolytic cell. All fatigue tests were conducted on a single machine under the same conditions at a stress ratio, R = 0.1, maximum stress = 256 MPa, and a frequency = 15 Hz. All the samples were analyzed after fracture to determine the exact location of crack initiation from a particular pit. The fracture surface was analyzed to obtain the crack parameters. The stress intensity factor for each sample was calculated using Newman–Raju approximation[16] and crack growth behavior was obtained through CRACK calculation[17].

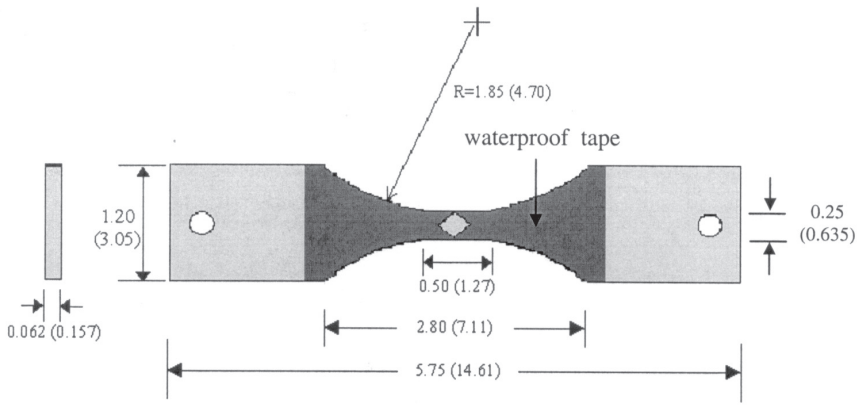

Figure 1. Geometry of dog-bone fatigue sample made of Al 2024-T3. Primary dimensions are in inches and dimensions in parentheses are in cm.

Results and Discussions

The controlled potentiostatic polarization scheme produced a wide range of pit sizes in a relatively short amount of time. For longer polarization times, larger and deeper pits were observed. The pit morphology was determined using WLIM. SEM was also used to characterize a few select samples. Since SEM is a well-established method, it was used to mainly compare the qualitative surface features with those shown in the WLIM surface profiles. Figure 2 shows a representative optical micrographs of a controlled pit created for one of the samples used in fatigue experiment.

A two-dimensional analysis was performed for each sample using WLIM. Figure 3 illustrates the two-dimensional analysis conducted to obtain pertinent pitting parameters, such as pit depth and pit diameter. Figure 3(a) shows the WLIM surface profile of representative pits created on a fatigue sample. In this analysis, the horizontal and vertical crossbars in (Figure 3(a)) are used in conjunction with (Figures 3(b) and (c)). The red horizontal crossbar in (Figure 3(a)) represents the X profile shown in (Figure 3(b)). This red crossbar can be maneuvered up and down over the entire surface to complete the scan in the X direction. Similarly the black and white triangular markers on (Figure 3(a)) correspond to those on the X profile in (Figure 3(b)). Figure 3(b) illustrates the measurement of the pit depth. The marker is moved to the bottom of the pit, and the exact Y coordinate is determined.

The Y profile shown in (Figure 3(c)) corresponds to the blue vertical line shown in (Figure 3(a)). The Y profile was used in the same manner as the X profile described earlier. Figure 3(c) illustrates the accurate determination of pit diameter. One marker is moved to the left side

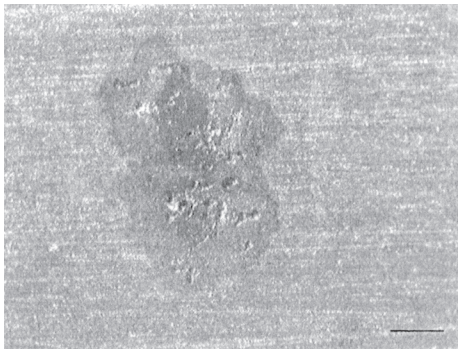

Figure 2. Optical micrograph of a controlled pit created on fatigue sample (X60).

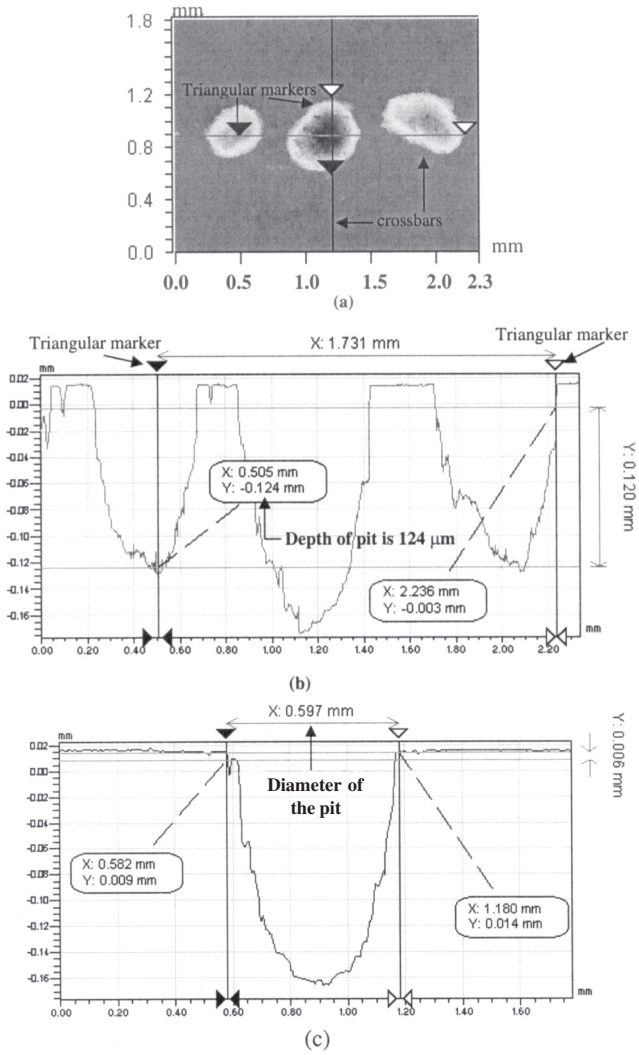

Figure 3. (a) Surface profile used in WLIM analysis. (b) X profile illustrating the determination of pit depth. (c) Y profile illustrating the determination of pit diameter.

of the pit mouth, while the other marker is moved to the right side of the pit mouth. The distance between these two points determines the pit diameter. All the required pit parameters for the analysis of fatigue data were determined using this analysis.

The pitted samples were fatigued after the surface pit morphology was characterized completely. The samples were fatigue tested at a stress ratio, R = 0.1 and a frequency, f = 15 Hz. The maximum stress in all cases was 256 MPa. The main goal was to determine a relationship between pit depth and stress intensity factor, K. The critical pit size is assumed as the size of the pit that initiates fatigue crack.

Figure 4 shows a representative picture of crack initiating from a pit after a number of fatigue cycles. The fracture surface of such a sample after failure is shown by SEM fractograph in (Figure 5). A detailed analysis of fracture surface indicated that crack always started from the pit at the corroded surface. In most cases the crack initiated from a single pit and a single semi-elliptical surface crack grew to a critical size leading to the failure of the specimen. In some cases, the cracks initiated from two or more adjacent pits. In these cases, the cracks linked together to form a single semi-elliptic crack that eventually caused the failure. The depth and diameter of this pit were calculated using the WLIM two-dimensional analysis. The number of pits on the specimen was very carefully controlled to a maximum of three. In this controlled set of experiments, the crack initiated mostly from the largest pit.

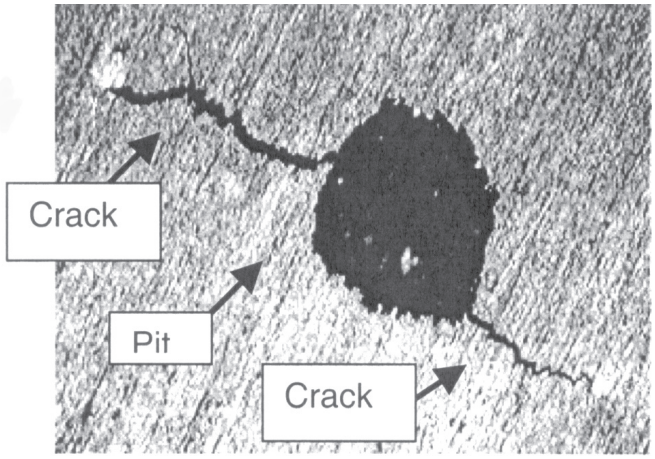

Figure 4. Large crack which initiated from a pit (X60).

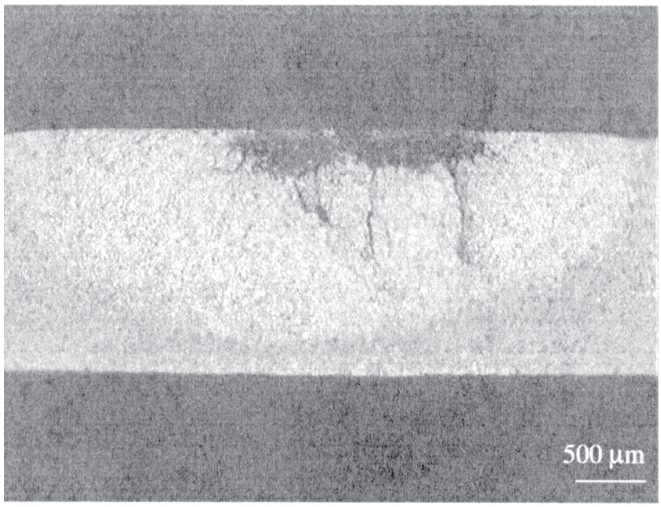

Figure 5. SEM fractograph of a fatigue sample after failure, showing semi-elliptical crack.

Figure 6 shows the dependence of fatigue life of the sample on pit depth. All tests were conducted at one maximum stress of 256 MPa. It is very clear from this figure that the fatigue life decreases with increase in pit depth initially in a sort of linear fashion, but a logarithmic trend is seen for deeper pits. More data is required before a meaningful model is attempted to predict fatigue life based on pit dimension. All the samples were examined as described above, and a complete list of the data is available[15]. Once the parameters of interest were obtained using WLIM, the stress intensity factor for each specimen was calculated. The stress intensity factor was used as the key fatigue parameter in developing a relationship between pit depth and fatigue parameter.

Figure 7 shows the crack geometry to elaborate the various parameters used in K calculation. W, here is the width of the specimen, 2c is the crack diameter, a is the crack length and β is the specimen thickness.

The stress intensity factor, K value for each sample was calculated using [Equation 1], where K is the initial stress intensity factor.

$$K = \beta\sigma\sqrt{\pi a} \qquad [1]$$

σ is the tensile stress and β is given by

$$\beta = Mg_1 f_\phi f_w f_x \qquad [2]$$

Again M, g, f_Φ, f_w and f_x are functions of a/t, a/t and Φ, a/c and Φ, a/t and W and c/a[16].

One of the main objectives of this study is to develop a relationship between a structural integrity parameter and a pitting parameter. Such a relationship is shown in (Figure 8). The stress intensity factor was plotted against critical pit depth. There appears to be a linear relationship between the two parameters. This relationship can be used to predict the life of structure. Fatigue crack growth model developed by University of Dayton Research Institute CRACKS model was used to predict the crack growth behavior of fatigue cracks initiating from a pit. A single semi-elliptical surface crack is assumed to develop from the critical pit. The model uses the stress intensity factor number from previous calculation and the crack growth data is generated from the initial and final crack size measured. Crack growth is assumed to start from the first applied cycle with no crack initiation period. Such an assumption is a reasonable approach because majority of the fatigue life of pitted sample comprises of growth stage[18].

The crack growth plot, ΔK vs da/dN is generated by the interpolation of tabular da/dN vs ΔK data for AA2024-T3 from[17]. Here N refers to number of fatigue cycle. ΔK is calculated as the difference between K_{max} and K_{min}. The first step in the determination of the value of K is the calculation of β. The operation starts with the initial crack length as a = a_0, and the crack length is allowed to grow in very small increments. The increment crack length is

$$a_{new} = a + da/dN \qquad [3]$$

At this point new values of β, ΔK and da/dN are calculated. In this manner, the crack is allowed to grow until it reaches the final size or $K_{max} = K_c$. The process of crack incremetation is iterated in a way such that the final crack length is identical with the crack length at the experimentally obtained crack length at fracture.

Crack growth data in the form of da/dN vs. stress intensity factor is shown in (Figure 9). The data shown as open squares are taken from notched compact tension specimen representing long crack growth[17]. The closed squares represent the data from pitted samples used in this study. It appears that the crack growth behavior of cracks initiating from pit is typical of short crack growth behavior. However, a transition to long crack growth behavior is quite evident suggesting that pits deeper than 80 μm behave similar to standard notched specimen representing long crack growth data. More tests are

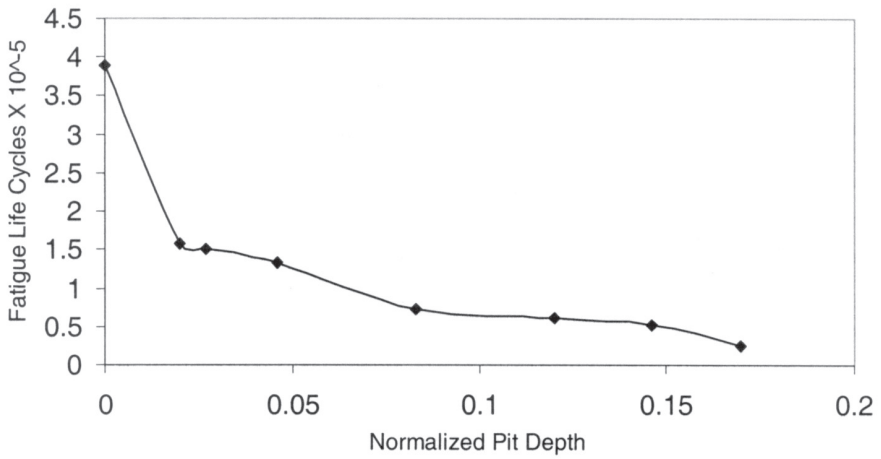

Figure 6. Dependence of fatigue life on normalized pit depth.

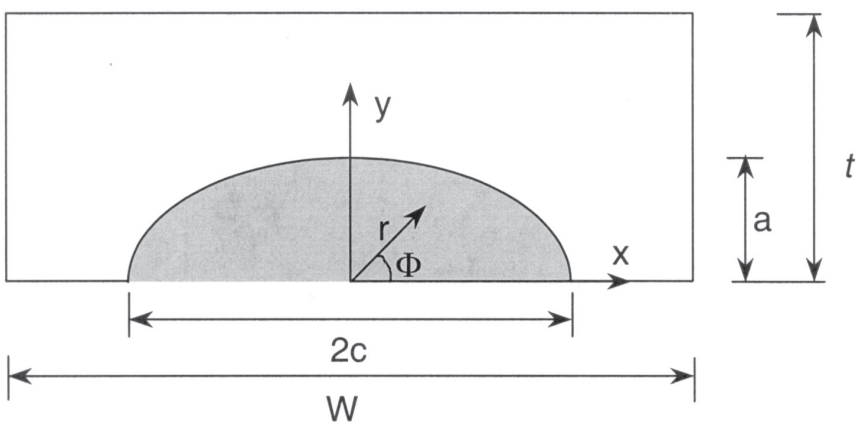

Figure 7. Schematics of crack geometry.

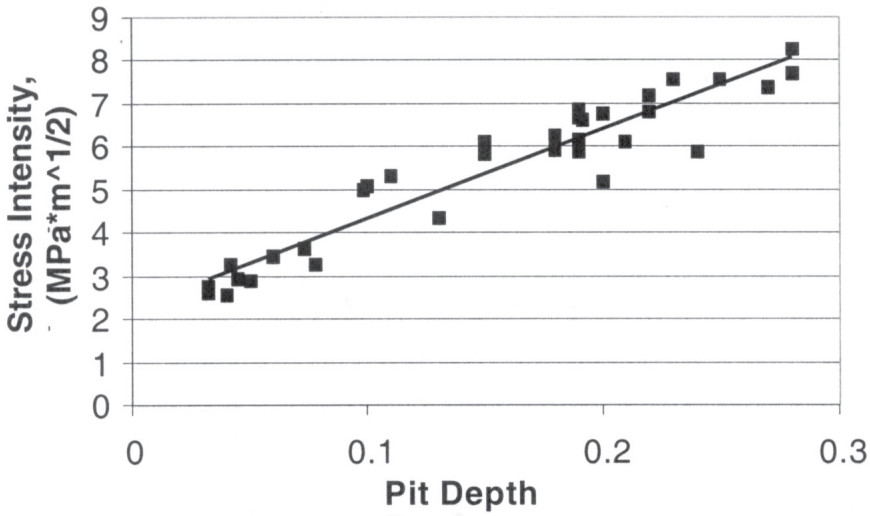

Figure 8. Stress intensity factor versus critical pit depth.

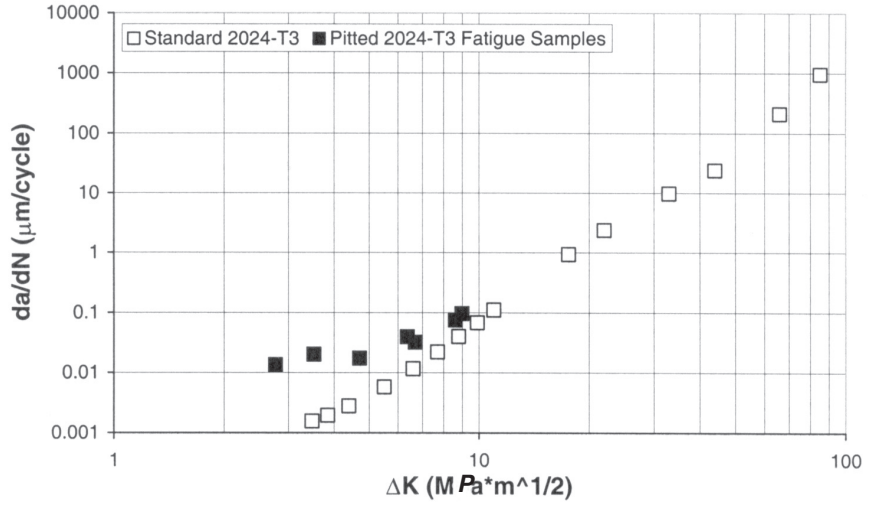

Figure 9. Crack-growth rate versus ΔK.

required with critical pit depths in the range of 100-200 μm.

Summary

A select number of pits were created on dog-bone fatigue sample by an electrochemical technique. The pit depth increased with increasing polarization time. All the pits were characterized using WLIM and SEM. Important parameters such as length and depth of the pits were determined. The fracture surface was analyzed to determine the initiation and failure locations on the surface. Stress intensity factors were calculated using pit parameters. A linear relationship was observed between critical pit depth and K. Fatigue crack growth initiating from a pit was observed to be typical of short crack. Sign of possible transition to long crack growth behavior was observed for pits deeper than 80 μm.

Acknowledgments

Effort sponsored by the Defense Advanced Projects Agency (DARPA) Multidisciplinary University Research Initiative (MURI), under Air Force Office of Scientific Research grant number F49620-96-1-0442. Technical assistance from Y. Ding, N. Schell, P.C. Mieldar and L. Simon are gratefully acknowledged.

References

1. S.I. Rokhlin, and J.Y. Kim, "Fracture Mechanical Analysis of Fatigue Crack Initiation and Growth from Pitting Corrosion," Second Annual Report for DARPA-MURI Under AFOSR Grant Number F49620-96-1-0442, p. A24-2, (1998).

2. John Alcott, "An Investigation of Nondestructive Inspection Equipment: Detecting Hidden Corrosion on USAF Aircraft," *Materials Evaluation*, p. 64, January (1994).

3. D.J. Groner, "US Air Force Aging Aircraft Corrosion," Current Awareness Bulletin, Structures Division, AFRL/FIBD, Aerospace Structures Information and Analysis Center, WPAFB, OH, Spring (1997).

4. R.J.H. Wanhill, "Aircraft Corrosion and Fatigue Damage Assessment," Proceedings of the US Air Force ASIP Conference, p. 9, San Antonio, TX, December (1995).

5. G.K. Cole, G. Clark, and P.K. Sharp, "The Implications of Corrosion with Respect to Aircraft Structural Integrity," Aeronautical and Maritime Research Laboratory, Melbourne, Australia, Research Report DSTO-PR-0102, AR-010-199, March (1997).

6. G.S. Chen, M. Gao, and R.P. Wei, "Microconstituent-Induced Pitting Corrosion in Aluminum Alloy 2024-T3," *Corrosion Science*, **Vol. 52**, No. 1, p. 8, (1996).

7. G.S. Chen, K.C. Wan, M. Gao, R.P. Wei, and T.H. Flournoy, "Transition for Pitting to Fatigue Crack Growth-Modeling of Corrosion Fatigue Crack Nucleation in a 2024-T3 Aluminum Alloy," *Materials Science and Engineering*, **Vol. A219**, p. 126, (1996).

8. R.S. Piascik, and S.A. Willard, "The Growth of Small Corrosion Fatigue Cracks in Alloy 2024," *Fatigue and Fracture of Engineering Materials and Structures*, **Vol. 17**, No. 11, pp. 1247-1248, (1994) .

9. S. Barter, P.K. Sharp, and G. Clark, "The Failure of an F/A-18 Trailing Edge Flap Hinge," *Engineering Failure Analysis*, **Vol. 1**, No. 4, p. 255, (1994).

10. W.W. Wallace, and D.W. Hoeppner, "AGARD Corrosion Handbook," Vol. 1, *Aircraft Corrosion: Causes and Case Histories*, AGARDograph No. 278, NATO, p. 101, July (1985).

11. R. Perez, "Metrics Exploration and Transformation Development for Corrosion/Fatigue," Final Report, Delivery Order 0005, USAF Contract F33615-95-D-3216, November (1996).

12. G. Mitchell, "Application of Corrosion Quantification Techniques to the USAF KC-135 Stratanker," *Proceedings of the Air Force 4th Aging Aircraft Conference*, p. 251, United States Air Force Academy, CO, July (1996).

13. M. Nakajima, and K. Tokaji, "A Mechanical Condition of Fatigue Crack Initiation from Corrosion Pits," Fatigue 1996, *Proceedings of the Sixth International Fatigue Congress*, Berlin, Germany, pp. 697-702, (1996).

14. E.P. Philips, and J.C. Neuman, "Impact of Small Crack Effect on Design Life Calculations," *Experimental Mechanics*, pp. 221-225, (1989).

15. L.B. Simon, "Influence of Pitting Corrosion on the Loss of Structural Integrity in Aluminum Alloy 2024-T3," Master's Thesis.

16. J.C. Newman, and I.S. J. Raju, "Stress-Intensity Factor Equations for Cracks in Three-Dimensional Finite Bodies," *Fracture Mechanics: Fourteenth Symposium*, Volume 1: Theory and Analysis. ASM STP 791, pp. I-238-I-265, (1983).

17. P.C. Miedler, and J.P. Gallagher, "Cracks 2000 Technical Guide," UDR-TR-2000-00136, University of Dayton, Dayton, OH.

18. G.H. Bray, R.J. Bucci, E.L. Colvin, and M. Kulak, "Effect of Prior Corrosion on the S/N Fatigue Performance of Aluminum Alloys 2024-T3 and 2524-T3," *Effects of the Environment on the Initiation of Crack Growth*, ASTM STP 1298, p. 89, (1997).